The Multiscale Factors Favorable for a Persistent Heavy Rain Event over Hainan Island in October 2010

WANG Huijie[1,2,4] (汪汇洁), SUN Jianhua[1,3*] (孙建华), ZHAO Sixiong[1] (赵思雄), and WEI Jie[1] (卫　捷)

1 *Key Laboratory of Cloud-Precipitation Physics and Severe Storms, Institute of Atmospheric Physics,*
Chinese Academy of Sciences, Beijing 100029

2 *Beijing Institute of Aeronautical Meteorology, Beijing* 100085

3 *Collaborative Innovation Center on Forecast and Evaluation of Meteorological Disasters,*
Nanjing University of Information Science & *Technology, Nanjing* 210044

4 *Meteorological Observatory, Unit 95959, Beijing* 100097

ABSTRACT

A case study is presented of the multiscale characteristics that produced the record-breaking persistent heavy rainfall event (PHRE) over Hainan Island, northern South China Sea (SCS), in autumn 2010. The study documents several key weather systems, from planetary scale to mesoscale, that contributed to the extreme rainfall during this event. The main findings of this study are as follows. First, the convectively active phase of the MJO was favorable for the establishment of a cyclonic circulation and the northward expansion of the Intertropical Convergence Zone (ITCZ). The active disturbances in the northward ITCZ helped direct abundant moisture from adjacent oceans towards Hainan Island continuously throughout the event, where it interacted with cold air from the midlatitudes and caused heavy rain. Second, the 8-day-long PHRE can be divided into three processes according to different synoptic systems: peripheral cloud clusters of a tropical depression-type disturbance over the central SCS in process 1; interactions between the abnormally far north ITCZ and the invading cold air in process 2; and the newly formed tropical depression near Hainan Island in process 3. In the relatively stable synoptic background of each process, meso-α- and meso-β-scale cloud clusters repeatedly traveled along the same path to Hainan Island. Finally, based on these analyses, a conceptual model is proposed for this type of PHRE in autumn over the northern SCS, which demonstrates the influences of multiscale systems.

Citation: Wang Huijie, Sun Jianhua, Zhao Sixiong, et al., 2016: The multiscale factors favorable for a persistent heavy rain event over Hainan Island in October 2010. *J. Meteor. Res.*, **30**(4), 496–512, doi: 10.1007/s13351-016-6005-2.

1. Introduction

Most of the rainfall events over East Asia occur in summer (Ding, 1992; Rasul et al., 2005; Zhao and Sun, 2007), whereas in tropical southeastern Asia south of 10°N, the majority of rainfall occurs during winter (Cheang, 1977; Wangwongchai et al., 2005). Hainan Island (18°–20.5°N, 108°–111.5°E) is located in the northern South China Sea (SCS), between the regions where these two monsoon rainfall regimes are dominant. In contrast, heavy rainfall frequently oc-curs over Hainan Island from June to October, and both precipitation amount and the number of rainy days peak in September and October. Similarly, heavy rainfall events frequently occur during the same period in northern Vietnam, which is at a similar latitude to Hainan Island (Yokoi and Matsumoto, 2008; Chen et al., 2012). This rainy period is known as the transition season from boreal summer monsoon to winter monsoon, during which the weather and precipitation are influenced by various meteorological systems that originate in both the tropical and mid-latitudes. How-

ever, few previous studies have examined such events.

In recent years, the duration of extreme precipitation events has been increasing at several places around the world (Kunkel et al., 1994, 1999; Bell and Janowiak, 1995; Grazzini and van der Grijin, 2003; Trenberth et al., 2003; Schumacher, 2011). Though heavy rainfall events over South China (Zhao et al., 2007) and the Yangtze–Huaihe valley (Bei et al., 2002) have been extensively studied, most studies of rainstorms over the SCS and the islands south of 20°N have focused on typhoon systems (Hogsett and Zhang, 2010; Wangwongchai et al., 2010), and only a few studies have investigated non-typhoon induced rainstorms (Qiao et al., 2015). Cheang (1977) observed that in the presence of cold surge, tropical disturbances could be intensified, which may cause winter rainfall in tropical southeastern Asia. Such cold surge vortices have been found in several heavy rainfall events around central Vietnam in autumn (Wu et al., 2011; Chen et al., 2012), and it was suggested that the cold surges without a tropical depression-type disturbance (TDD) would not lead to much precipitation (Yokoi and Matsumoto, 2008).

Persistent heavy rainfall events (PHREs) often occur in a quasi-stationary circulation pattern, when the synoptic- and meso-scale systems are in the same area or are traveling along the same path, resulting in significant cumulative rainfall (Ding, 1994). It has been shown that slow-moving or stationary blocking highs remain stable to the west and east of Eurasia in mid and high latitudes, respectively, whereas the western Pacific subtropical high (WPSH), which is stronger in lower latitudes, causes upstream frontal systems to move slowly, which favors continuous torrential rain from April to June in Guangdong, South China (Xie et al., 2006). However, the mechanisms behind the appearance of PHREs in autumn have not been clarified yet; these events need to be studied further.

According to the PHRE definition by Wang et al. (2014a), a PHRE occurred from 30 September to 8 October 2010 over the whole Hainan Island, as well as northeastern Indochina Peninsula and adjacent seas (Fig. 1a); this event is the subject of this research. The peak rainfall during this event reached 701.9 mm

day^{-1} on 5 October 2010, which led to the most severe flood recorded in the past 50 years at Qionghai meteorological station (Fig. 1a). This calamitous flood event inundated more than 1160 villages, affected 1.65 million people in 16 cities and counties, and resulted in approximately 168.77 million U.S. dollars of direct economic loss (Wang, 2010).

In this study, two scientific problems are investigated: (1) How can the PHRE sustain for a long time period during the retreat of the summer monsoon over the SCS? (2) What meteorological systems on different scales influenced the three processes of the PHRE? The remainder of the paper is organized as follows. The datasets and methods are described in Section 2. Section 3 presents the general circulation features of the PHRE, and Section 4 explores the multiscale systems of the three processes during the PHRE. Conclusions and a conceptual model of the type of PHRE occurring over Hainan in autumn are provided in Section 5.

2. Data and methods

The primary rainfall data used in this study were the hourly precipitation from surface observation stations in China provided by the China Meteorological Administration, and Tropical Rainfall Measuring Mission (TRMM) 3B42RT v6 rainfall estimates (Huffman et al., 2007) at 3-h intervals and a resolution of 0.25° × 0.25°. We also used TBB (temperature of black body) data (both daily and 3-h intervals) from the Fengyun (FY)-2E satellite with a horizontal resolution of 0.1° × 0.1°, and hourly TBB data from GSM-IR with a horizontal resolution of 0.05° × 0.05°. The climatological geopotential height was derived based on the daily NCEP–NCAR reanalysis data at a 2.5° × 2.5° resolution from 1981 to 2010. All other analyses and diagnoses were performed based on the NCEP final reanalysis data at 6-h intervals and at 1° × 1° horizontal grids. Additionally, GDAS (Global Data Assimilation System) data (Kanamitsu, 1989), at 6-h intervals and a horizontal resolution of 1° × 1°, were used to compute backward trajectories.

The backward Lagrangian trajectories were calcu-

lated by using the HYSPLIT (Hybrid Single-Particle Lagrangian Integrated Trajectory) model (Draxler and Hess, 1998) to reveal the source locations of different currents. Based on the Lagrangian trajectories, trajectory cluster analysis was conducted, by which similar trajectories were grouped together. In this study, each member of a cluster of backward trajectories was computed from the same source location, but the original meteorological grid is offset by ± 1 grid point in both the meridional and zonal directions. The center point is located at 19°N, 110°E, which is very close to the geometric center of Hainan Island. Two calculation schemes that differed in terms of altitude and duration were adopted in this study. The first scheme calculated backward trajectories starting from 500-, 1000-, and 1500-m altitudes for 168 h (i.e., 7 days) from 0000 UTC 30 September to 1800 UTC 7 October to track the moisture sources and transport pathways. The second scheme calculated backward trajectories starting from altitudes of 500, 1500, and 3000 m for 72 h (i.e., 3 days) to depict the pertinent weather systems. For the first scheme, the moisture transport contribution ratio was defined as follows:

$$Q_s = \frac{\sum\limits_1^m q_{\text{last}}}{\sum\limits_1^n q_{\text{last}}} \times 100\%, \qquad (1)$$

where Q_s is the moisture transport contribution rate of each cluster, q_{last} is the specific humidity at the final location of each trajectory, m is the number of trajectories in each cluster, and n is the total number of trajectories computed.

3. General circulation features of the PHRE

3.1 The synoptic weather pattern

The total precipitation during the PHRE from 30 September to 8 October over Hainan Island and its surroundings is given in Fig. 1a. There are two main precipitation maxima: one greater than 800 mm along the Annam Range over central Vietnam, and the other of 1462.2 mm in Qionghai along the eastern coast of Hainan Island. Extreme rainfall occurred over much of Hainan's eastern coast, with cumulative precipita-

tion amounts of 1385.4 mm in Wenchang, 1182.5 mm in Wanning, and 930.2 mm in Lingshui.

Given the evolution of synoptic circulation and the location of the precipitation, the PHRE was divided into three precipitation processes. The first process was from 30 September to 2 October, with local precipitation occurring over the southeastern coast of Hainan Island. The second process lasted from 3 to 5 October, when successive periods of torrential rainfall took place across the entire island, with a maximum precipitation center located in the eastern coastal area. The third process was from 1200 UTC 5 to 0000 UTC 9 October, with a torrential rainstorm on the northeastern island. From observational precipitation recorded at representative stations, it can be seen that heavy rainfall occurred at Lingshui in process 1 (Fig. 1b), torrential rainfall struck Qionghai in process 2 (Fig. 1c), and heavy rain fell at Wenchang in process 3 (Fig. 1d). In addition, the rainfall during the second and third processes was much more intense than that during the first process.

The mean 200-hPa geopotential height and height anomaly during 30 September–9 October show an omega block extending from eastern Europe to central Asia (Fig. 2a). The core of the blocking high was positioned over northern Europe, and its flanking trough was over Siberia, with a stationary cut-off low located over the Black Sea. The intensities of both the blocking high and the cut-off low were extraordinary. The South Asian high (SAH) extended from the Arabian Sea to the Philippine Islands and had a center anomaly of +2.0 stretching from the southern SCS to the western Maritime Continent, which caused Hainan Island to be influenced by the southeastward movement of the cold flow. However, a deep trough over East China also developed downstream, with a center anomaly of +1.5 situated to the east of the Philippines. The mean standardized anomalies of the large-scale systems around Hainan Island all reached a level above 1.0, suggesting a sustained anomaly circulation, which was similar to the pattern observed at 500 hPa (Fig. 2b). The remarkable development of both the SAH and the deep trough over East China prevented the adjacent synoptic systems from moving
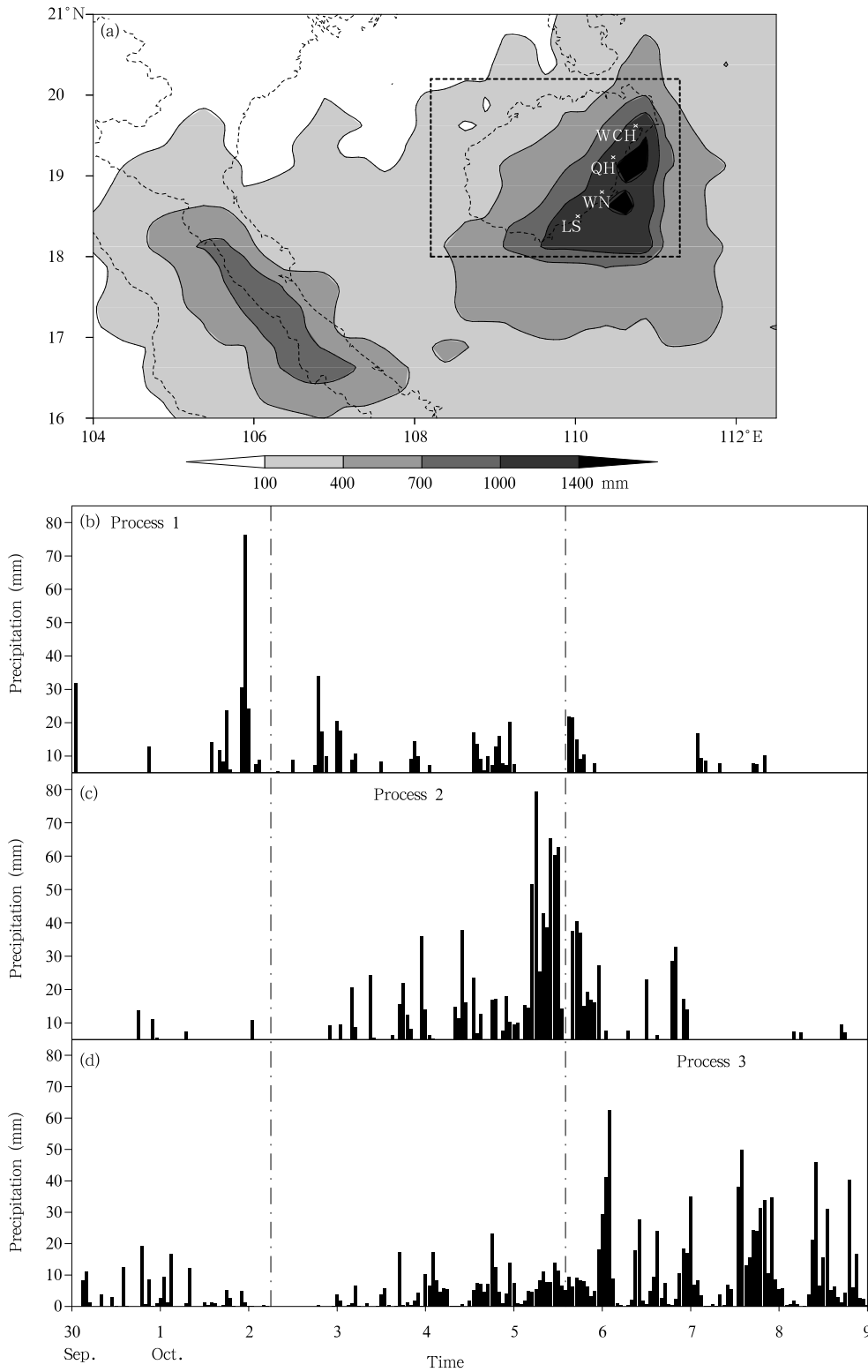
Fig. 1. (a) Total precipitation amount (mm) from TRMM from 0000 UTC 30 September to 9 October 2010 and hourly precipitation amount (mm) from rain gauges from 0000 UTC 30 September to 9 October 2010 at (b) Lingshui (LS), (c) Qionghai (QH), and (d) Wenchang (WCH). WN in (a) means Wanning.
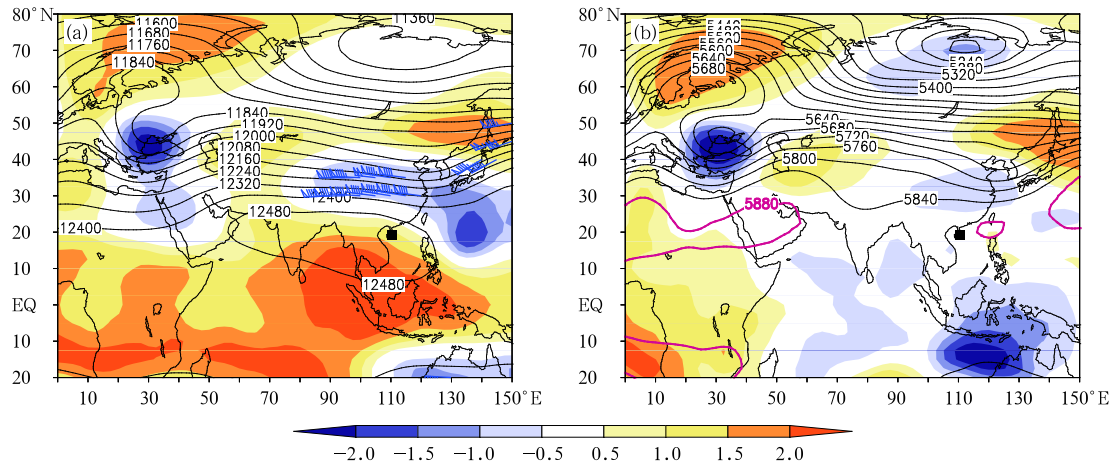
Fig. 2. Mean geopotential height (solid lines; gpm) and anomaly relative to climatological mean (color-shaded; gpm) between 0000 UTC 30 September and 9 October 2010 at (a) 200 hPa (blue wind barbs depict the upper-level jet) and (b) 500 hPa. The location of Hainan Island is marked with a black square.

downstream, which favored the maintenance of the circulation pattern. Moreover, the WPSH at 500 hPa was abnormally weak and extended mainly over central Pacific, with its western edge located to the east of 120°E. The upper-level jet and shortwave troughs at 500 hPa over central China favored the southward invasion of cold air. The stable mid- and high-latitude circulations favored persistent heavy rainfall over Hainan Island, but the activity of tropical systems was more important to the occurrence of the PHRE.

3.2 *Intraseasonal oscillation and the ITCZ with disturbances*

Wavelet analysis of the regional averaged OLR data (Fig. 3) suggests that an 8–14-day oscillation dominated between September and mid November. A 30–40-day oscillation was also active in September and October, although the 8–14-day oscillation is statistically more significant than the 30–40-day oscillation, which is in agreement with the results of Qiao et al.
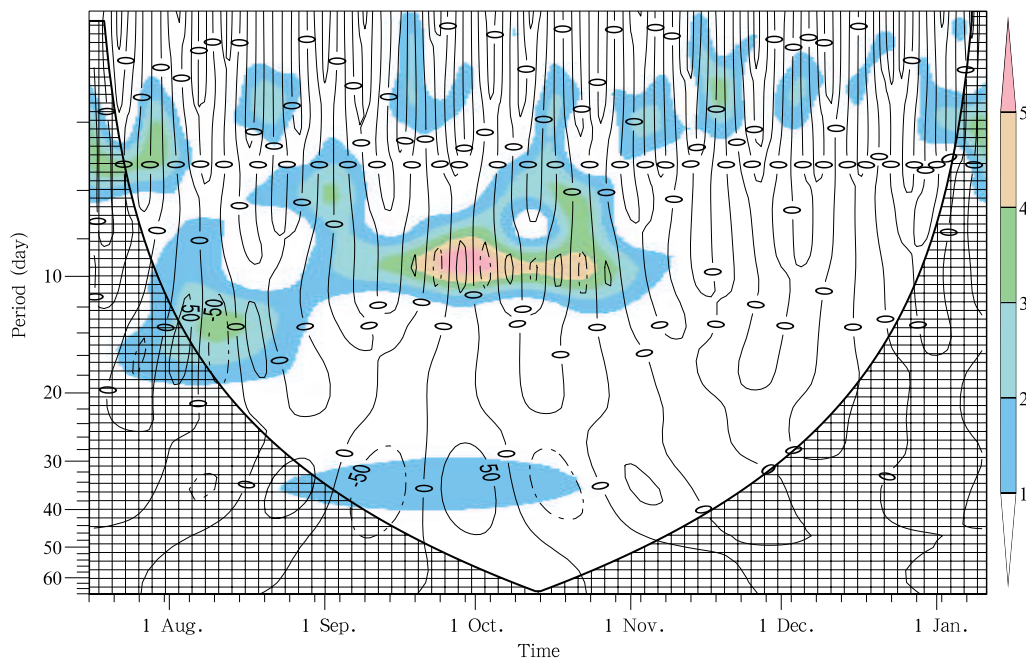

Fig. 3. Wavelet analysis of OLR. The isolines represent the wavelet transform coefficients, and the color-shaded regions are above the 5% significance level.

(2015). The observations from the Hainan Island PHRE are, to a certain extent, similar to the convective propagation observed in autumn in same latitudes (Yokoi et al., 2007; Chen et al., 2012). The contribution from the two intraseasonal modes to the convective propagation can be illustrated by the time series of filtered zonal winds. These time series are made by applying a Butterworth bandpass filter (Murakami, 1979) to the two modes for zonal wind (850 hPa) at different locations. The two intraseasonal modes exhibited coincident maximum values of easterly anomalies at 20°N (Fig. 4a) on approximately 3–5 October; the maximum zonal wind speeds also occurred at 20°N during this period. Meanwhile, the westerly anomalies at 10°N (Fig. 4b) reached their maximum values in both the 8–14-day mode and the zonal wind speed, but the maximum speeds were only approximately -1 m s^{-1} in the 30–40-day mode, which is half of that observed in the 8–14-day mode. The peak easterly anomalies to the north and westerly anomalies to the

south of Hainan Island clearly indicate that the maximum wind of certain cyclonic circulations was established mainly by the intraseasonal modulation of the 8–14-day mode.

A Hovmöller diagram of TBB in Fig. 5a (averaged between 5°N and 5°S) shows that the tropical convection during the study period was dominated by the occurrence of an MJO convection envelope, with an envelope of enhanced convection amplifying over the Indian Ocean during late September to early October, then moving eastward into the western Pacific Ocean (WPO) with suppression. Further, as the Hovmöller diagram of TBB averaged between 20° and 5°N (Fig. 5b) indicates, to the north of the tropical region, cloud clusters with scales of hundreds of kilometers propagated westward at approximately 12-day intervals from the Maritime Continent and the WPO, which shows an intraseasonal oscillation (ISO). These two oscillations became amplified over the SCS, where both the tropical eastward convection and extratropi-
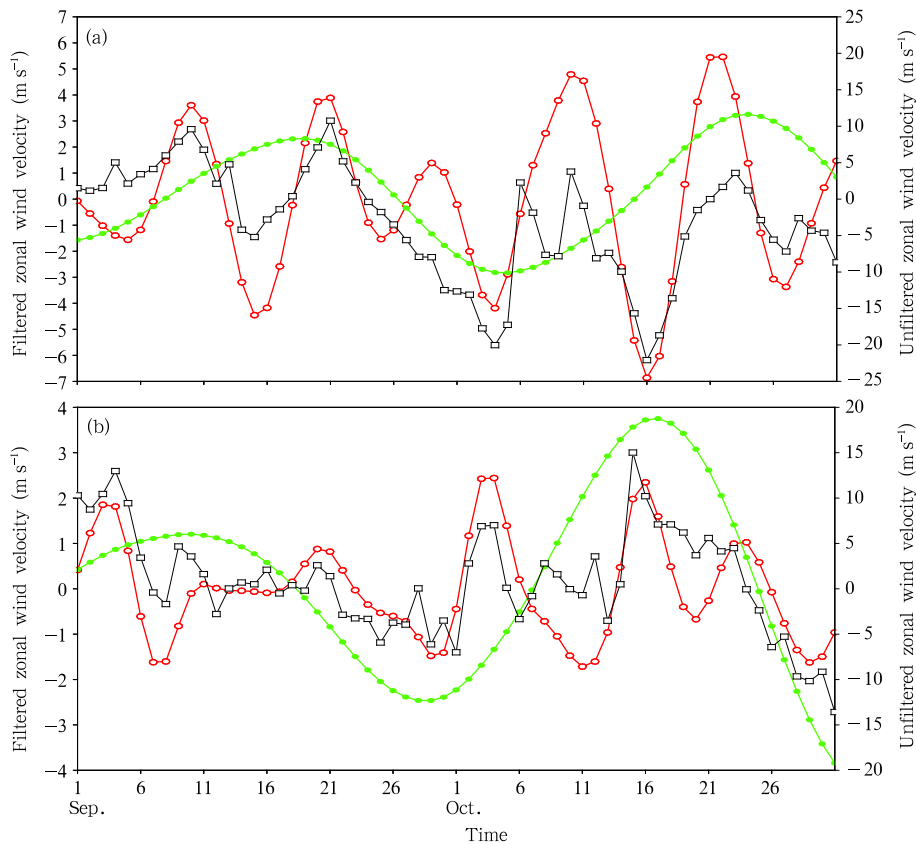

Fig. 4. Time series for zonal wind (black line), 8–14-day mode of zonal wind (red line), and 30–40-day mode of zonal wind (green line) at (a) 20°N, 110°E and (b) 10°N, 110°E.
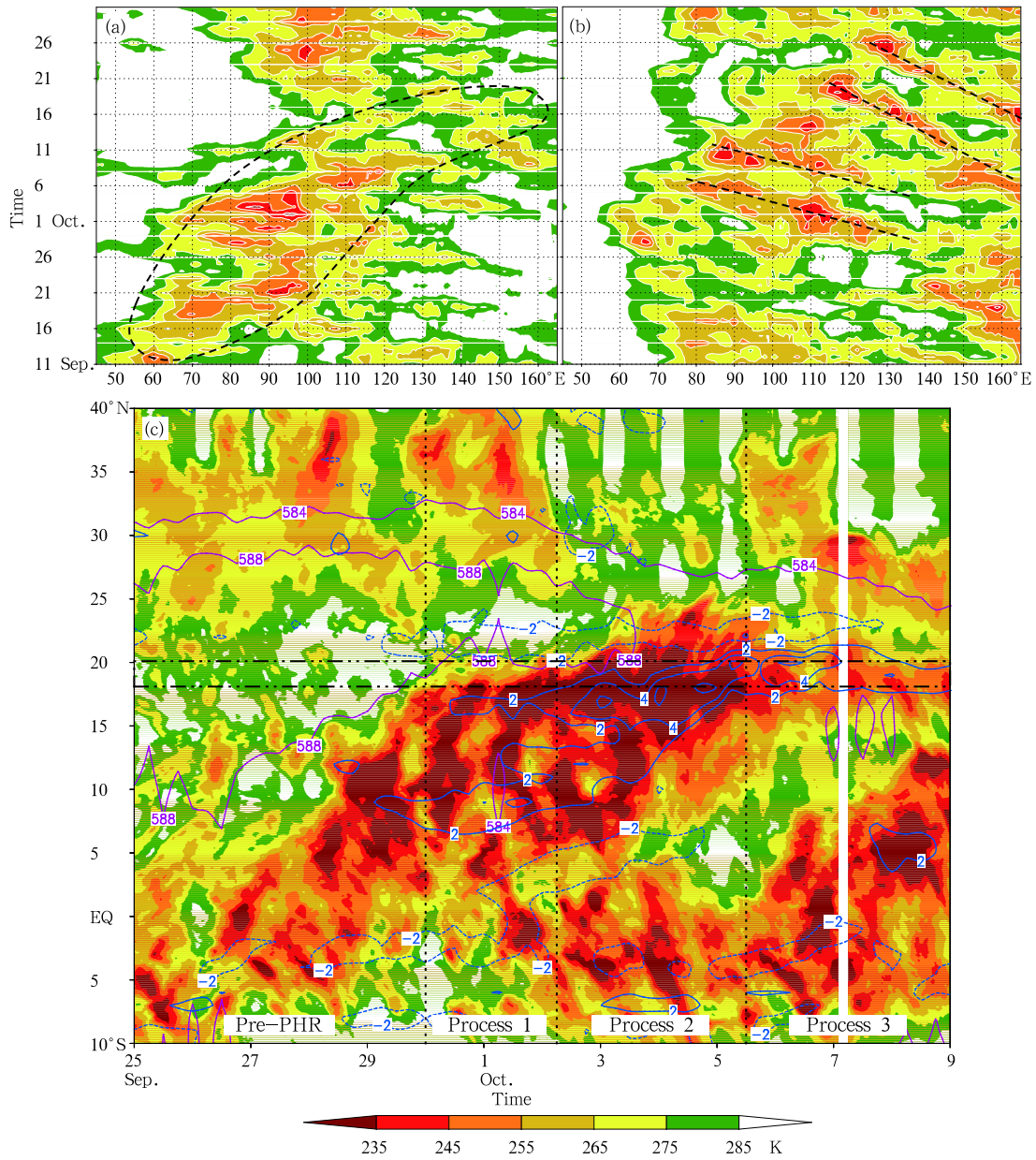
Fig. 5. Time-longitude diagrams of averaged TBB (K) for the period 11 September to 31 October 2010 between (a) 5°N and 5°S (a significant MJO is enclosed by the black dashed line), and (b) 20° and 5°N (dotted lines emphasize the westward ISO). (c) Time-latitude cross-section of mean TBB (color shaded; with missing data between 0300 and 0500 UTC 7 October; K), mean vertical vorticity at 850 hPa (blue lines; 10^{-5} s^{-1}) between 105° and 115°E, and mean geopotential height at 500 hPa (bold lines in purple; dagpm) between 110° and 120°E, where bold long-and-short dashed lines in black outline the location of Hainan Island, and bold dotted lines in black outline the processes of the event.

cal westward convection arrived during late September to early October. Therefore, ITCZ convection over the SCS appears to be reinforced by these two oscillations.

To reveal the development of tropical disturbances and other systems, a time-latitude cross-section of the mean TBB field, geopotential height at 500 hPa,

and vorticity at 850 hPa between 105° and 115°E are shown in Fig. 5c. Notably, before this PHRE, South China, including Hainan Island, was under the influence of the WPSH. Then, the WPSH retreated eastward and narrowed progressively. Meanwhile, the ITCZ (with embedded disturbances) moved northward

and gradually widened, becoming active. During process 1, the southern margin of the WPSH reached 20°N, where it matched the northern edge of the ITCZ, with a positive vorticity maximum moving northward. During process 2, the WPSH retreated to the WPO, while the northern edge of the ITCZ approached north of 20°N and its positive vorticity maximum intensified to 4×10^{-5} s^{-1}, which favored the formation and intensification of the tropical depression (TD) in process 3. For example, the TBB based on FY-2E data and 850-hPa streamline field at 0000 UTC 1 October (figure omitted) depict a series of vortices and disturbances in the off-equator tropical area of Asia, which indicates the activity of the ITCZ (Gadgil and Guruprasad, 1990). At the end of process 3, as the disturbances were depressed, the ITCZ retreated southward and weakened, and the WPSH moved back to the SCS.

3.3 Trajectory analysis and moisture transportation

Undoubtedly, continuous moisture transport plays an important role in the maintenance of PHREs. The computation from the Lagrangian scheme described in Section 2 revealed the existence of five paths (Fig. 6a): path 1 from Lake Baikal; path 2 from the WPO; path 3 from the SCS; path 4 from Sumatra; and path 5 from the East China Sea. As depicted in Figs. 6b and 6c, all of the paths transported moisture below 800 hPa except path 1, which originated over Lake Baikal at 650 hPa and had little moisture content, indicating the transfer of cold and dry air that did not become wetter until it flowed over coastal areas in lower latitudes. Paths 2–4 all traced back to tropical oceans, which have lower altitude and higher moisture content, whereas path 5 originated from the midlatitude ocean with a specific humidity of 8 g kg^{-1}. The air parcels along all five paths became higher and wetter just 12 h before they arrived at central Hainan, which transported moisture to the PHRE region. As shown in Fig. 6d, the moisture contribution ratios of each path estimated from the HYSPLIT model were nearly equal, except that of path 1, which carried cold and dry air from the trough at Lake Baikal (Fig. 2b).
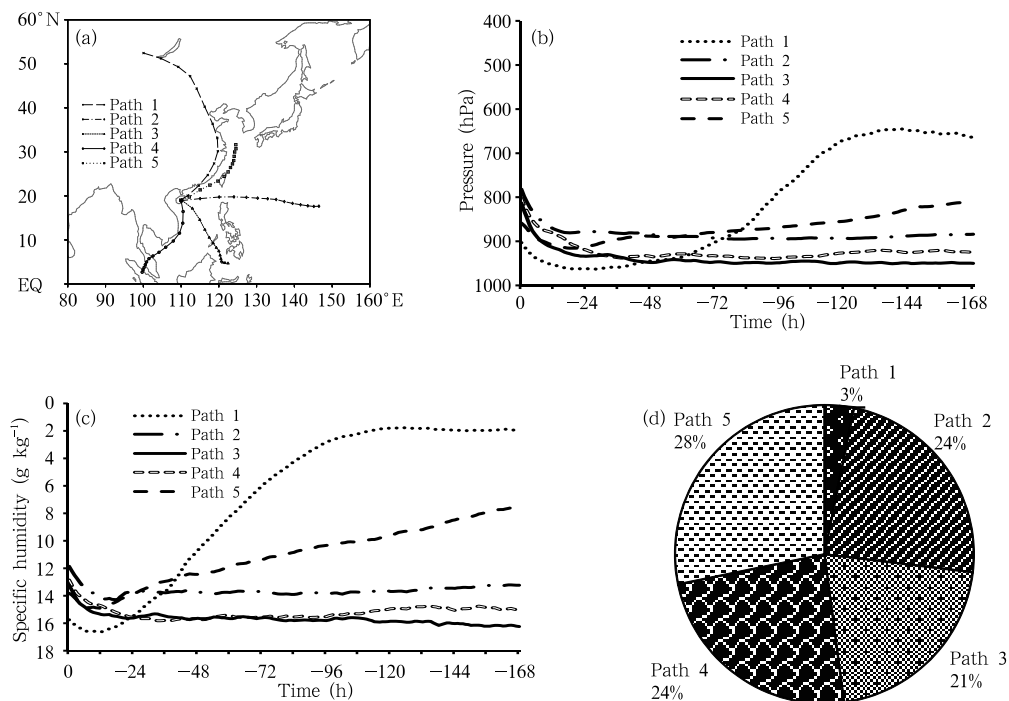

Fig. 6. (a) Horizontal distribution of moisture sources and their backward paths for 168 h. The vertical distribution of every path of 168-h backward moisture transport by using (b) pressure (hPa) and (c) specific humidity (g kg^{-1}) coordinates. (d) The moisture transport contribution ratio of five paths (%).

The majority of the moisture supply came from the tropics and subtropics.

As mentioned above, the large-scale circulation favorable for the PHRE included the exceptionally strong and stationary blocking highs over northern Europe, with the main trough over Siberia, and the eastward-moving shortwave trough promoting the southward invasion of cold air. Meanwhile, the PHRE occurred during the convectively active phases of the 8–14- and 30–40-day oscillations in the tropics, which favored the establishment of cyclonic circulation and the northward expansion of the ITCZ, and led to significant interactions between mid- and low-latitude systems. Moisture from the WPO, the SCS, Sumatra, and the East China Sea converged over Hainan Island in similar proportions, and the majority of moisture came from the tropical oceans at lower latitudes.

4. The multiscale systems of three processes during the PHRE

The three main processes during the PHRE were influenced by similar global circulation patterns. However, there were different synoptic-scale as well as mesoscale convective systems during different processes. To illustrate the three-dimensional structure of these systems, the mean stream field at 850 hPa and mean vertical cross-sections for various processes of moisture flux, temperature, pseudo-equivalent potential temperature (θ_{se}), as well as vertical circulation, are all given in Fig. 7.

4.1 Process 1: Peripheral cloud clusters of the TDD over central SCS

Before process 1 (from 30 September to 2 October), as the meridional component of equatorial southeasterlies in the Southern Hemisphere (SH) intensified, the cross-equatorial flow (CEF) emerged and turned to southwesterly flow after crossing the equator into the Northern Hemisphere (NH), which grew stronger with time. On 30 September, the southwestern flow met the eastern flow over the central SCS, which was responsible for the formation of the TDD during process 1. Simultaneously, both the southwestern flow and the eastern flow intensified due to the cyclonic genesis.

Hainan Island was influenced by the easterly flow to the north of the disturbance (Fig. 7a). Moisture from the whole column converged over Hainan Island. From the vertical cross-section (Fig. 7b), a maximum moisture flux of greater than 15 g hPa^{-1} cm^{-1} s^{-1} up to 800 hPa, with strong updraft of the whole column, between 17° and 21°N, can be found over Hainan Island. In addition, θ_{se} decreased with height, and the low-value region in the vertical column extended deeply from 800 to 400 hPa, which indicates arising convective instability. Meanwhile, a frontal zone was located near 30°N, far north of Hainan Island, which implies a cold surge from the midlatitudes. To the north of the frontal zone, an anticyclone existed from 925 to 700 hPa (Fig. 7a). The 72-h backward trajectories (Fig. 8b) confirm this cold air invasion: air parcels mainly originated at heights between 300 and 1200 m and exhibited anticyclonic trajectories along the coast of the East China Sea. The moisture content of this cluster increased significantly when air parcels traveled southward into the SCS (Fig. 6c).

However, during this process, nearly 80% of the trajectories traveled westward from the WPO (Fig. 8a), under the influence of peripheral convective clouds of the TDD over the central SCS (Fig. 7a). Four peripheral cloud clusters with TBB of –60℃ propagated eastward over the southern island, each with a horizontal scale of 300–600 km (Fig. 9a). The meso-β convective system with TBB of –80℃ in the meso-α cloud cluster arrived over Lingshui at 2200 UTC (Fig. 9b), which contributed to the precipitation peak of 76.3 mm h^{-1} at 2300 UTC 1 October (Fig. 1b).

4.2 Process 2: Northward movement of the ITCZ and invasion of cold air

During process 2 (from 3 to 5 October), the ITCZ extended from the Bay of Bengal to the northern SCS (Fig. 7c). Essentially, the ITCZ was located over the southern SCS rather than the central and northern SCS, which is unusual in autumn (Waliser and Gautier, 1993). Four currents, i.e., the southward shift of cold air from North China (Fig. 8c), the moist southerly current from the SCS (Fig. 8d), the southeasterly from Sumatra (Fig. 8e), and the easterly flow from the WPO (Fig. 8f), gathered over Hainan Island
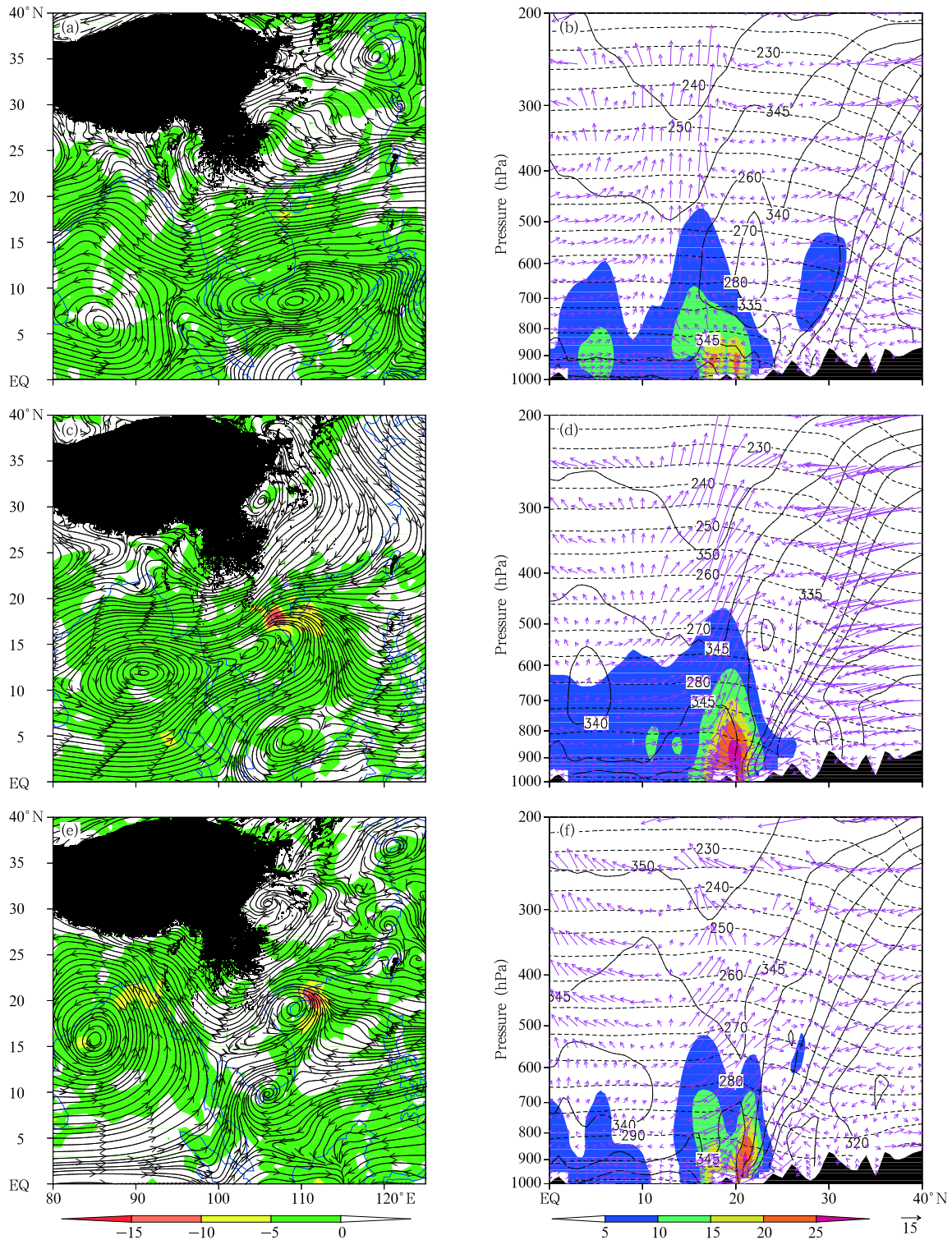
Fig. 7. Mean stream field at 850 hPa and mean divergence of horizontal moisture flux in the whole column (color-shaded; 10^{-4} kg m^{-2} s^{-1}) during (a) process 1, (c) process 2, and (e) process 3. High terrain is colored black. Mean vertical cross-section of moisture flux (color-shaded; g hPa^{-1} cm^{-1} s^{-1}), temperature (dashed lines; K), pseudo-equivalent potential temperature (solid lines; K), and vertical circulation (vectors; m s^{-1}, with vertical velocity multiplied by 100) along 110°E during (b) process 1, (d) process 2, and (f) process 3. Black regions represent the terrain.
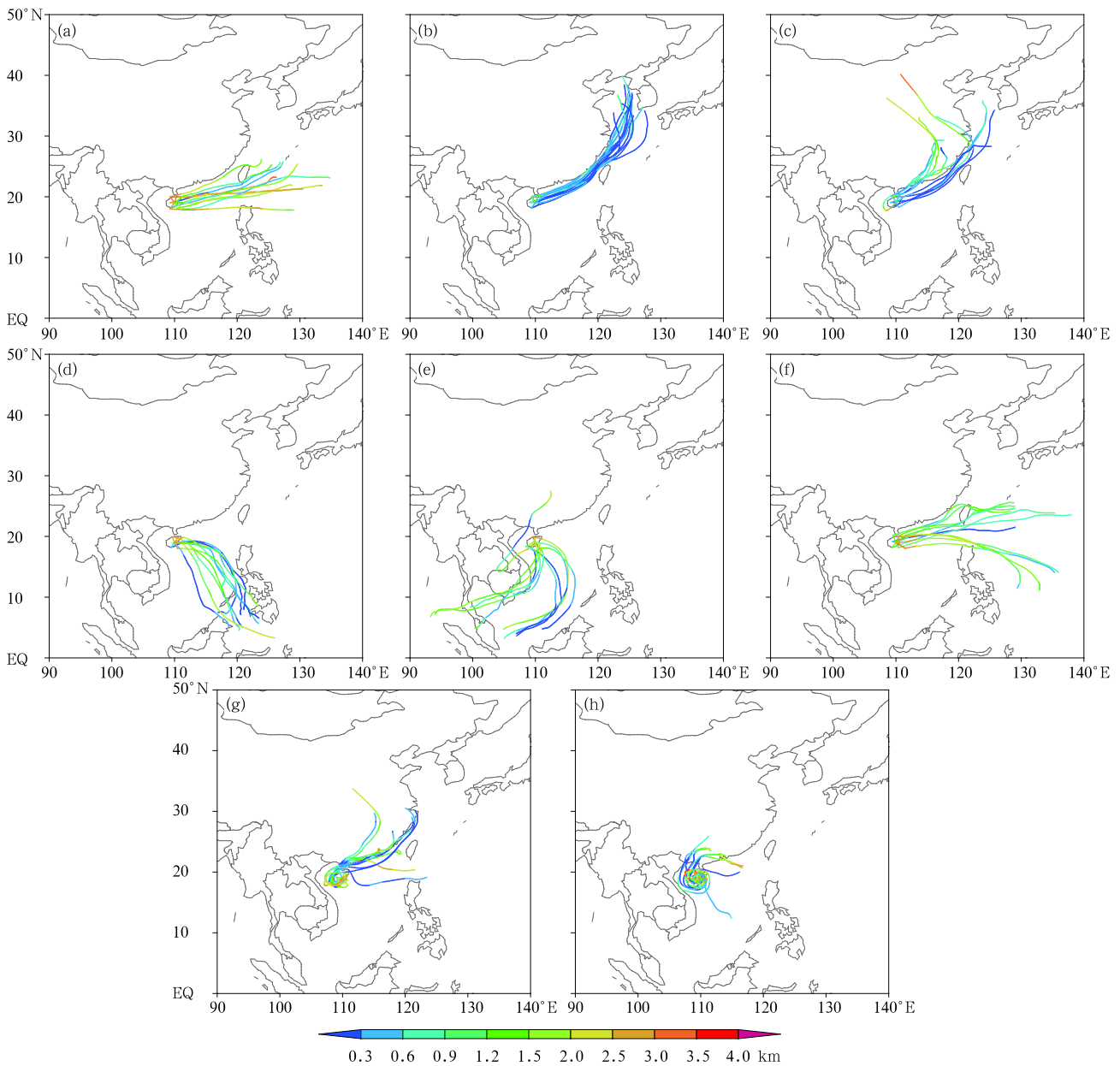
Fig. 8. Trajectories of each cluster during (a, b) process 1, (c–f) process 2, and (g, h) process 3. The colors represent the height (km) of air parcels.

and the Beibu Gulf, thereby significantly enhancing the moisture convergence. The northward moisture transport was strengthened during this process by the northward movement of the ITCZ, and the northward and northeastward trajectories corresponded to the disturbances in the ITCZ (Fig. 7c). Therefore, the trajectories from the WPO also decreased from 80% to 27%. The frontal zone in the lower troposphere had

already approached 20°N (Fig. 7d), which became an influential system, as did the ITCZ. Neutral stratification appeared in the mid and lower troposphere, resulting from the strong convective activity. The higher θ_{se} than that in the surrounding area implies the existence of a warmer core in the mid troposphere.

Notably, the mainland of China was dominated by a high-pressure system at 0000 UTC 5 October (figure

omitted) with three maxima: the southern one located over Fujian Province, with a central pressure of 1021 hPa, which is typical in winter but rare in autumn over China; the western one over central China, with a maximum of 1023 hPa; and the eastern one over northeastern China, with a central pressure of 1018 hPa. These correspond to the source points of the trajectories (Fig. 8c). Meanwhile, due to the deep trough to the east of Sichuan basin at 500 hPa (Fig. 2b), with shortwave troughs downstream, cold air moved southward. A comparison of thermal advection between 950 and 850 hPa (figure omitted) indicates that cold advection extended to the center of Hainan Island at 950 hPa, with a maximum of -4×10^5 K m s^{-2} at 1200 UTC 4 October. Meanwhile, at 850 hPa, cold advection propagated to the northern edge of Hainan Island and turned into warm advection after 4 October, which indicates that the layer of cold air invasion was quite thin. Cold air parcels originated between 500 and 4000 m in elevation, descended along the trajectory, and arrived over Hainan Island at a height of 500–1500 m (Fig. 8c). The altitude of trajectories originating from central China was much higher than that of the others. It can also be seen in Fig. 7d that both moisture flux and updraft over Hainan Island were stronger than those in process 1. The increasing gradient of isolines of θ_{se} to the north of Hainan Island indicates the significant influence of frontogenesis.

During process 2, there were three meso-α cloud clusters passing over Hainan Island (figure omitted); according to the northward movement of the ITCZ, the horizontal scale of these clusters covered the whole island (Fig. 9b), just over the frontal area. The 24-h precipitation on 5 October 2010 reached 701.9 mm at Qionghai and 392.2 mm at Wanning, both were record-breaking events. The severe rainfall was high because of the development of mesoscale convective systems. Wang et al. (2014b) showed a linear echo greater than 40 dBZ located only along the eastern coast of Hainan Island (Fig. 10a) during this time, and it was caused by a mesoscale convergence line formed as the easterly wind was affected by the topography of the eastern coast (Fig. 10b). Along the linear echo, several meso-γ convective cells were found near Qionghai, where the

rainfall intensity reached 79.4 mm h^{-1} at 0600 UTC, and a total rainfall of 701.9 mm on 5 October was reported. Wang et al. (2014b) also indicated that the mesoscale topography in the middle of Hainan Island is favorable for the formation and maintenance of mesoscale convective systems when they move close to the northeastern slope, because the flow of moist air over the topography is characterized by a moderate Froude number.

4.3　Process 3: Formation and maintenance of the TD

During process 3 (from 1200 UTC 5 to 0000 UTC 9 October), the easterly low-level jet dissipated, the cold air weakened, cold air parcels originated from below 2500-m altitude (Fig. 8g), and the frontal zone decreased significantly (Fig. 7f). Nevertheless, the moisture convergence remained, which led to the appearance of the new TD-caused rainstorms over Hainan Island. The new TD separated from the ITCZ and stayed over Hainan Island for the rest of the process, with strong moisture convergence (Fig. 7e) and meso-β convective clusters with TBB of -70℃ (Fig. 9b) in the northeastern sector of the depression, where several torrential rainstorms occurred over the northeastern Hainan Island. A vortex extended over Hainan Island, with an intense updraft and a strong moisture flux in the northeast quadrant (Fig. 7f). Backward trajectories depict the spiral flow of the TD: peripheral air parcels descended gradually, and central air parcels ascended rapidly (Fig. 8h). Fu et al. (2011) characterized the long-lived TD in process 3 from an energy dynamics perspective and suggested that intense convergence in the lower troposphere, the vertical transport of positive vorticity, and the barotropic energy conversion, all contributed to the longevity of the vortex. However, that study did not consider the contributions of multiscale systems and interactions between mid- and low-latitude systems.

5.　Conclusions and discussion

In this study, a record-breaking PHRE that was caused by the interaction of systems of different spatial and temporal scales, from both mid- and low-latitude,
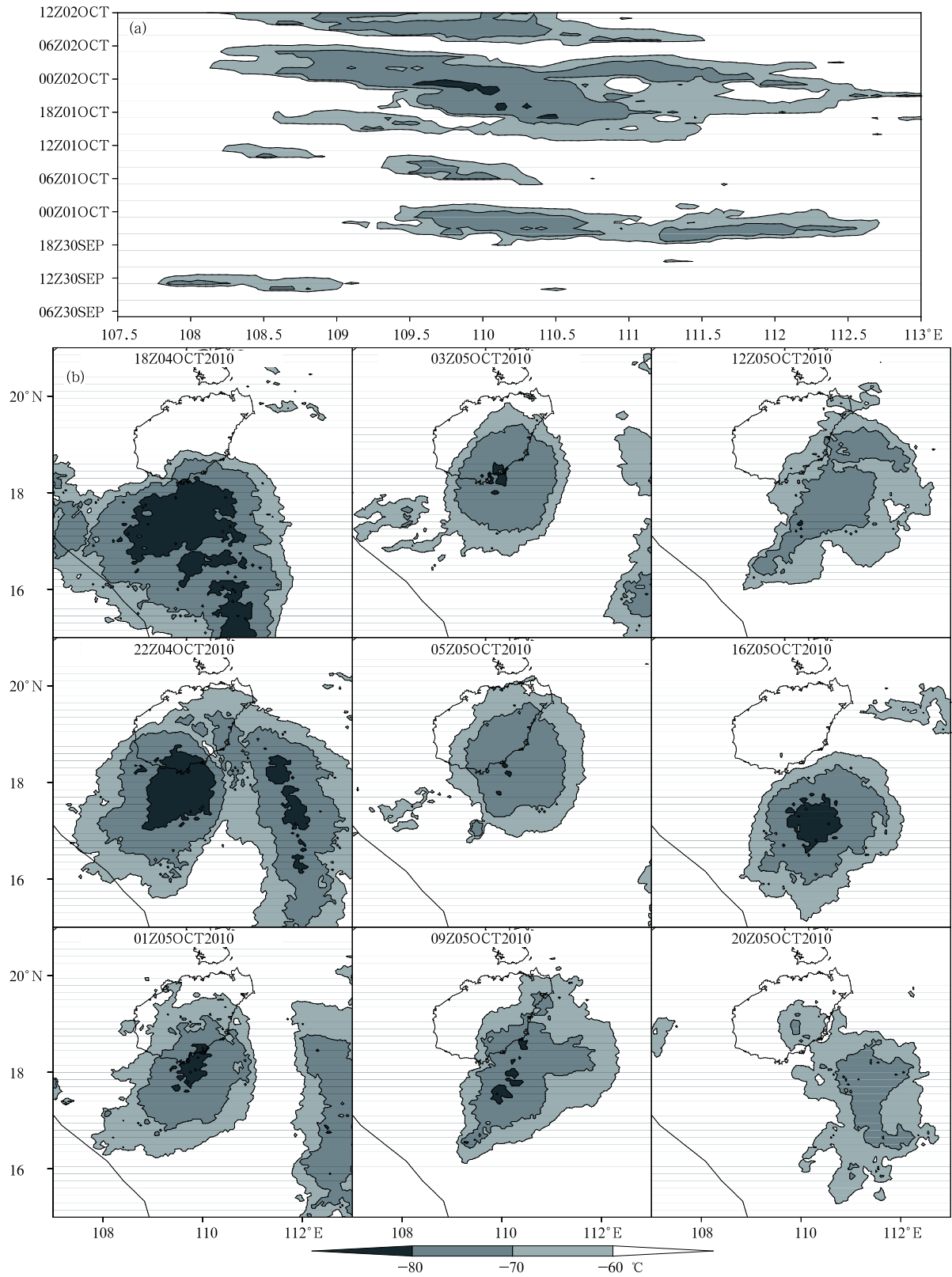
Fig. 9. (a) Longitude-time section of hourly TBB at 18.5°N from 30 September to 2 October 2010. (b) Horizontal distributions of convective clusters with TBB below –60℃, columns from left to right depict processes 1, 2, and 3, respectively.
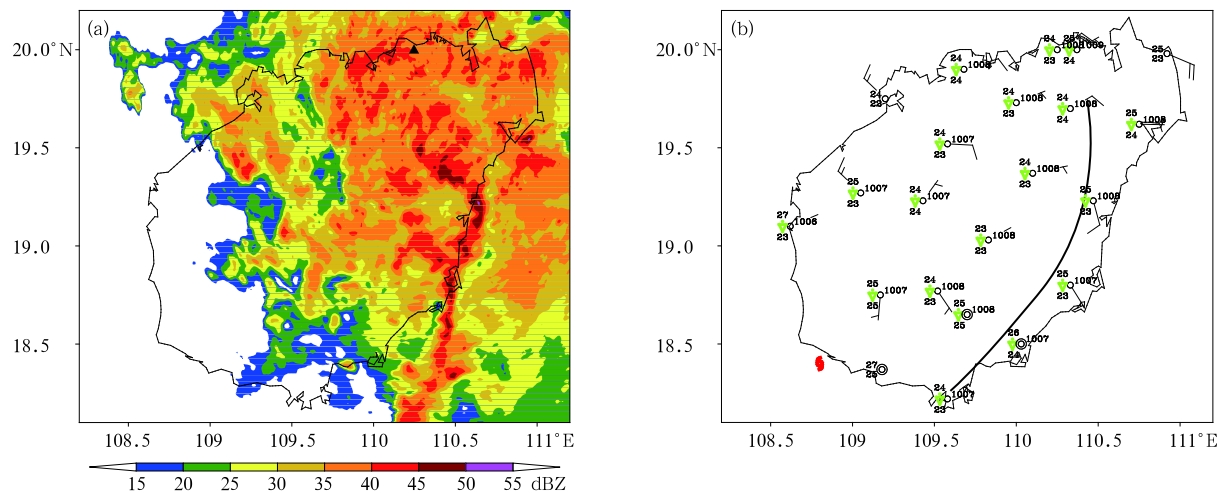
Fig. 10. (a) Composite reflectivity observed by radar in Haikou (marked with black triangle) at 0602 UTC 5 October and (b) surface observation at 0600 UTC 5 October (full barb = 4 m s^{-1}). The brown line in (b) denotes the shear line.

during 30 September–8 October 2010, was investigated. The following conclusions can be drawn.

(1) In the midlatitudes, the blocking pattern and westerly trough with a closed low over Lake Baikal were stable. The intense cold airflow from shortwave troughs in North China invaded southward, which is rare in autumn. The PHRE occurred during the convectively active phase of the MJO. The active ITCZ extended uncommonly far north (for autumn) to the northern SCS, thereby favoring convective development, which may provide an explanation for the persistence of the rainfall.

(2) The air parcel trajectories, which were derived by using a Lagrangian scheme, revealed five paths of air parcels sourced from Lake Baikal, the WPO, the SCS, Sumatra, and the East China Sea. Our analysis of the moisture contribution ratios indicates that the majority of moisture came from the tropical ocean at lower latitudes.

(3) This PHRE was caused by a weak TDD in the ITCZ and a long-lasting small-scale TD, which indicates that the conditions were favorable for sustaining the storms rather than for further development of the TD. Therefore, special attention should be given to weak TDDs in autumn, which appear frequently over the northern SCS.

(4) Built on previous work, a conceptual model of this type of PHREs over Hainan Island in autumn

is proposed (Fig. 11). The sustained, very strong blocking high over northern Europe and the trough over central Siberia at 500 hPa favor the southward invasion of cold air. The cold front shifts southward to almost 20°N, north of Hainan Island. In low latitudes, the northward movement of the ITCZ with embedded disturbances, the southwest current, the northward-moving cross-equatorial flow near 105°E, and the newly developing TD, are all favorable elements for a long-duration PHRE. Because of the complex large-scale circulation, mesoscale convective systems form along the eastern coastal region and are organized by a mesoscale convergence line associated with the easterly wind and the island's topography. Therefore, frequent PHREs in autumn over Hainan Island is a result of the interactions not only between mid- and low-latitude systems but also between the NH and the SH, which are too complex to be analyzed with one case. Other cases should be studied in future research.

A conceptual model of this type of PHRE occurring in autumn over the northern SCS is proposed. More attention should be paid to the interactions during PHREs in weather forecasts for Hainan Island and in the northern SCS. The similarities and differences of this model and some previous low-latitude heavy rainfall models were also examined. The model in this study is quite different from the model of rainstorms
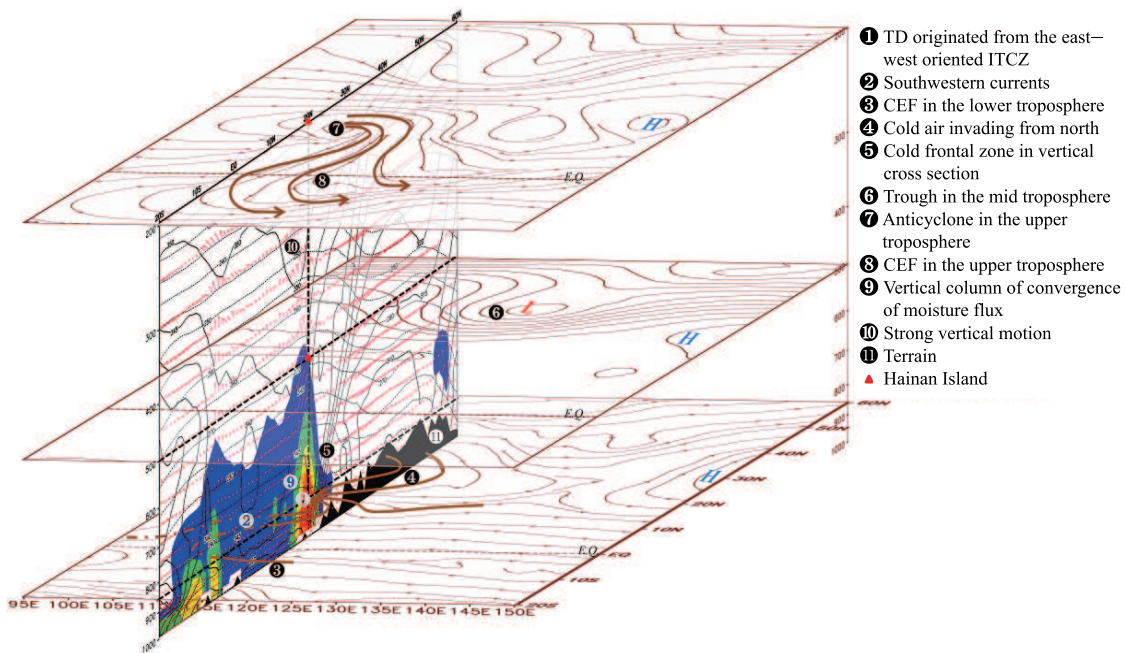
Fig. 11. Conceptual model of this type of PHRE occurring in autumn over Hainan Island.

caused by the monsoon trough over South Asia, which occurs without invading cold air (Rasul et al., 2005), though the monsoon trough in South China is occasionally identified as the ITCZ. It is also different from the model of the heavy rainfall caused by convection in the warm sector ahead of a front during the pre-rainy season in South China, which occurs with few depressions (Zhao et al., 2007). The model in this study is more complex because it is not associated with a single occurrence of heavy rainfall, but is instead composed of multiple systems and processes.

In addition, autumn is a transitional season when the summer monsoon diminishes and the winter monsoon begins to set up over the SCS, which may involve rapidly changing weather systems, and their variation and impact are quite difficult to predict and estimate. It must be noted that there are many different types of PHREs in autumn over Hainan Island, and it is impossible to discuss them in one paper or evaluate them in one study. In this work, several scientific problems are studied and discussed in terms of the multiscale aspects of the influencing systems, and the interactions between mid- and low-latitude systems involved in this PHRE, with insightful results obtained. However, some phenomena are not yet understood in

sufficient depth, such as the feedback of mesoscale convection to the longevity of the large-scale background, and the influence of other factors such as topography and sharp contrasts in land–sea atmospheric conditions. These topics are beyond the scope of this paper but will be discussed in future work.

REFERENCES

Bei, N. F., S. X. Zhao, and S. T. Gao, 2002: Numerical simulation of a heavy rainfall event in China during July 1998. *Meteor. Atmos. Phys.*, **80**, 153–164, doi: 10.1007/s007030200022.

Bell, G. D., and J. E. Janowiak, 1995: Atmospheric circulation associated with the Midwest floods of 1993. *Bull. Amer. Meteor. Soc.*, **76**, 681–695, doi: 10.1175/1520-0477(1995)076<0681:ACAWTM>2.0.CO;2.

Cheang, B. K., 1977: Synoptic features and structures of some equatorial vortices over the South China Sea in the Malaysian region during the winter monsoon,

December 1973. *Pure Appl. Geophys.*, **115**, 1303–1333, doi: 10.1007/BF00874411.

Chen, T. C., M. C. Yen, J. D. Tsay, et al., 2012: Synoptic development of the Hanoi heavy rainfall event of 30–31 October 2008: Multiple-scale processes. *Mon. Wea. Rev.*, **140**, 1219–1240, doi: 10.1175/MWR-D-11-00111.1.

Ding, Y. H., 1992: Summer monsoon rainfalls in China. *J. Meteor. Soc. Japan*, **70**, 373–396.

Ding Yihui, 1994: Some aspects of rainstorm and mesoscale meteorology. *Acta Meteor. Sinica*, **52**, 274–284, doi: 10.11676/qxxb1994.036. (in Chinese)

Draxler, R. R., and G. Hess, 1998: An overview of the HYSPLIT_4 modeling system for trajectories. *Aust. Meteor. Mag.*, **47**, 295–308.

Fu, S. M., W. L. Li, J. H. Sun, et al., 2011: A budget analysis of a long-lived tropical mesoscale vortex over Hainan in October 2010. *Meteor. Atmos. Phys.*, **114**, 51–65, doi: 10.1007/s00703-011-0156-6.

Gadgil, S., and A. Guruprasad, 1990: An objective method for the identification of the Intertropical Convergence Zone. *J. Climate*, **3**, 558–567, doi: 10.1175/1520-0442(1990)003.

Grazzini, F., and G. van der Grijn, 2003: Central European Floods during Summer 2002. ECMWF Newsletter No. 96, United Kingdom, ECMWF, 18–28.

Hogsett, W., and D. L. Zhang, 2010: Genesis of Typhoon Chanchu (2006) from a westerly wind burst associated with the MJO. Part I: Evolution of a vertically tilted precursor vortex. *J. Atmos. Sci.*, **67**, 3774–3792, doi: 10.1175/2010JAS3446.1.

Huffman, G. J., R. F. Adler, D. T. Bolvin, et al., 2007: The TRMM Multisatellite Precipitation Analysis (TMPA): Quasi-global, multiyear, combined-sensor precipitation estimates on fine scales. *J. Hydrometeor.*, **8**, 38–55, doi: 10.1175/JHM560.1.

Kanamitsu, M., 1989: Description of the NMC global data assimilation and forecast system. *Wea. Forecasting*, **4**, 335–342, doi: 10.1175/1520-0434(1989)004.

Kunkel, K. E., S. A. Changnon, and J. R. Angel, 1994: Climatic aspects of the 1993 upper Mississippi River basin flood. *Bull. Amer. Meteor. Soc.*, **75**, 811–822, doi: 10.1175/1520-0477(1994)075.

Kunkel, K. E., K. Andsager, and D. R. Easterling, 1999: Long-term trends in extreme precipitation events over the conterminous United States and Canada.

J. Climate, **12**, 2515–2527, doi: 10.1175/1520-0442(1999)012.

Murakami, M, 1979: Large-scale aspects of deep convective activity over the GATE area. *Mon. Wea. Rev.*, **107**, 994–1013, doi: 10.1175/1520-0493(1979)107<0994:LSAODC>2.0.CO;2.

Qiao Yunting, Zhang Chunhua, and Jian Maoqiu, 2015: Role of the 10–20-day oscillation in sustained rainstorms over Hainan, China in October 2010. *Adv. Atmos. Sci.*, **32**, 363–374, doi: 10.1007/s00376-014-3200-x.

Rasul, G., Q.-U.-Z. Chaudhry, Zhao Sixiong, et al., 2005: A diagnostic study of heavy rainfall in Karachi due to merging of a mesoscale low and a diffused tropical depression during South Asian summer monsoon. *Adv. Atmos. Sci.*, **22**, 375–391, doi: 10.1007/BF02918751.

Schumacher, R. S., 2011: Ensemble-based analysis of factors leading to the development of a multiday warm-season heavy rain event. *Mon. Wea. Rev.*, **139**, 3016–3035, doi: 10.1175/MWR-D-10-05022.1.

Trenberth, K. E., A. Dai, R. M. Rasmussen, et al., 2003: The changing character of precipitation. *Bull. Amer. Meteor. Soc.*, **84**, 1205–1217, doi: 10.1175/BAMS-84-9-1205.

Waliser, D. E., and C. Gautier, 1993: A satellite-derived climatology of the ITCZ. *J. Climate*, **6**, 2162–2174, doi: 10.1175/1520-0442(1993)006 <2162:ASDCOT>2.0.CO;2.

Wang Huijie, Sun Jianhua, Wei Jie, et al., 2014a: Classification of persistent heavy rainfall events over southern China during recent 30 years. *Climatic Environ. Res.*, **19**, 713–725, doi: 10.3878/j.issn.1006–9585.2013.13143. (in Chinese)

Wang Huijie, Sun Jianhua, Zhao Sixiong, et al., 2014b: A mesoscale study of extreme rainfall along the eastern coast of Hainan Island in October 2010. *J. Trop. Meteor.*, **30**, 518–532, doi: 10.3969/j.issn.1004-4965.2014.03.013. (in Chinese)

Wang, Q., 2010: More rain forecast for Hainan. China Daily, (2010-10-08). Available online at http://www.chinadaily.com.cn/cndy/2010-10/08/content_11382414.htm.

Wangwongchai, A., Zhao Sixiong, and Zeng Qingcun, 2005: A case study on a strong tropical disturbance and record heavy rainfall in Hat Yai, Thailand during the winter monsoon. *Adv. Atmos. Sci.*, **22**, 436–450, doi: 10.1007/BF02918757.

Wangwongchai, A., Zhao Sixiong, and Zeng Qingcun, 2010: An analysis of Typhoon Chanthu in June 2004 with focus on the impact on Thailand. *Adv. Atmos. Sci.*, **22**, 14–32, doi: 10.1007/s00376-009-8206-4.

Wu, P. M., Y. Fukutomi, and J. Matsumoto, 2011: An observational study of the extremely heavy rain event in northern Vietnam during 30 October–1 November 2008. *J. Meteor. Soc. Japan*, **89A**, 331–344, doi: 10.2151/jmsj.2011-A23.

Xie Jiongguang, Ji Zhongping, Gu Dejun, et al., 2006: The climatic background and medium-range circulation features of continuous torrential rain from April to June in Guangdong. *J. Appl. Meteor. Sci.*, **17**, 354–362. (in Chinese)

Yokoi, S., and J. Matsumoto, 2008: Collaborative effects of cold surge and tropical depression-type disturbance on heavy rainfall in central Vietnam. *Mon. Wea. Rev.*, **136**, 3275–3287, doi: 10.1175/2008MWR2456.1.

Yokoi, S., T. Satomura, and J. Matsumoto, 2007: Climatological characteristics of the intraseasonal variation of precipitation over the Indochina Peninsula. *J. Climate*, **20**, 5301–5315, doi: 10.1175/2007JCLI1357.1.

Zhao, S. X., and J. H. Sun, 2007: Study on cut-off low-pressure systems with floods over Northeast Asia. *Meteor. Atmos. Phys.*, **96**, 159–180, doi: 10.1007/s00703-006-0226-3.

Zhao Sixiong, Bei Naifang, and Sun Jianhua, 2007: Mesoscale analysis of a heavy rainfall event over Hong Kong during a pre-rainy season in South China. *Adv. Atmos. Sci.*, **24**, 555–572, doi: 10.1007/s00376-007-0555-2.